

Size effect in structural high strength concrete

G. Appa Rao

Department of Civil Engineering, IITM, Chennai, India.

B.K. Raghu Prasad

Department of Civil Engineering, IISc., Bangalore, India.

ABSTRACT: Determination of true size effect in high strength concrete (HSC) is very important. Moreover, a comprehensive study of the same is also of utmost important when wide variables such as geometry and other influencing factors are included. This paper, therefore, enumerates some experimental and analytical studies to understand the type of size effect in high strength concrete structures. Different geometries are adopted to distinguish the nature of size effect law. Experimental observations shows that a complex size effect on strength of HSC exists in direct tension using double edge notch compact tension specimens (DENCTS), while strong size effect has been observed in HSC using eccentric compact compression specimens (ECCS) and three-point bend beam (TPB) specimens. Relatively large size specimens are needed to achieve general size effect in direct tension. A characteristic size of 210 mm seems to be the smallest size to observe size effect in direct tension. The size of fracture process zone (FPZ) in HSC has been analyzed. The effect of geometry on size effect has been analyzed using the extent of FPZ in the crack tip regions.

1. INTRODUCTION

Several fracture mechanics models have been proposed to characterize the failure of concrete (Hillerborg et al. 1976; Jenq and Shah 1989; Bazant and Oh 1984, Karihaloo, 1995). Each of these models introduces some material fracture properties regardless of geometry and size of the structure. Fracture of concrete structures exhibits a size effect, which has been explained as a consequence of the randomness of material strength. According to Bazant whenever the failure does not occur at the initiation of cracking, the size effect should properly be explained by energy release caused by macro-crack growth. Bazant's size effect law (Bazant and Oh 1984) is based on the ductile-brittle transition of the failure mode of geometrically similar fracture specimens. In linear elastic fracture mechanics (LEFM), the whole fracture process is assumed to take place in front of the crack tip. According to LEFM, the normal stress, σ_N decreases in proportion to square root of depth of specimen, $d^{-1/2}$. Hence the plot of $\log(\sigma_N)$ versus $\log(d)$ is an inclined line with a slope of $-1/2$. However, in concrete structures, the size effect is transitional between the strength criterion representing horizontal line and the size effect of LEFM represented by the inclined line. The size

effect in high strength concrete needs to be understood further, particularly because HSC tends to be relatively brittle. The question is whether HSC with strength greater than 60 MPa, behaves more according to the principles of LEFM. Is size effect more pronounced in HSC? These questions will be clarified through the discussions in the paper. Bazant's size effect law can be described by equation 1.

$$\sigma_N = Bf_0 \left(\frac{1}{\sqrt{1 + \frac{d}{d_0}}} \right) = Bf_0 (1 + \beta)^{-\frac{1}{2}} \quad (1)$$

Where f_N or σ_N = Nominal strength, d = size of the specimen, $\beta = d/d_0$, B and d_0 are empirical parameters to be determined using experimental data.

2. EXPERIMENTAL PROGRAM

2.1. Materials and mix proportioning

Ordinary Portland cement was used with silica fume obtained commercially. Sand was passing through 2.36mm obtained from natural source and

the coarse aggregate was crushed granite. A constant water-cement ratio of 0.30 was used throughout the program. In order to improve the workability of concrete, a naphthalene sulphonate type super plasticizer was incorporated at 5-8 lit/m³ of concrete. A total of twelve mixes were selected, while changing various parameters such as the maximum size of coarse aggregate, the cement content and coarse aggregate content. These concrete mixes are grouped as A, B and C. Details are given in Table 1 for DENCTS.

Table 1: Quantities of constituent materials in various concrete mixes

Mix	d _a mm	Cement (kg/m ³)	Sand (kg/m ³)	CA (kg/m ³)
410-A	10	390	779	1169
416-A	16	390	779	1169
420-A	20	390	779	1169
415-A	M	390	779	1169
460-B	10	425	756	1134
466-B	16	425	756	1134
470-B	20	425	756	1134
465-B	M	425	756	1134
510-C	10	459	734	1101
516-C	16	459	734	1101
520-C	20	459	734	1101
515-C	M	459	734	1101

The compressive strength of concrete used for ECCS was 66.7 MPa. The tensile strength was 5.0 MPa. The concrete mix proportions were 1:1.29:2.14 with a water-cement ratio of 0.35. The cement content was 510 kg/m³ using 20 mm size coarse aggregate. No silica fume was used. Further, three-point bend (TPB) specimens have also been adopted to study the influence of type of specimen on the type of size effect of high strength concrete. The compressive strength of concrete was 74 MPa and the tensile strength was 5.0 MPa. The mix proportions were 1:1.56:2:0.30. Cement with 10 % silica fume content was 477 kg/m³ in the concrete mix with 12.5 mm coarse aggregate.

2.2. Test specimens

The dimension of all DENCTS in the third direction was constant at 80 mm. The length to depth ratio was maintained at 2.0. The notch to depth ratio was 0.32. The depth of different double edge notched specimens were 80 mm, 110 mm, 200 mm and 225 mm. Uniaxial tension tests were specially undertaken for understanding the general behavior of HSC in tension. In the case of

ECCS, four different sizes were adopted viz. 100 mm x 100 mm x 200 mm, 100 mm x 150 mm x 300 mm, 100 mm x 200 mm x 400 mm and 100 mm x 300 mm x 600 mm, at a constant edge notch-to-depth ratio of 0.25 on both the edges of the specimen. The dimensions of the beam specimens, TPB, were: 100 mm x 50 mm x 250 mm, 100 mm x 100 mm x 500 mm and 100 mm x 150 mm x 750 mm with notch-to-depth ratio of 0.33 in all the beams. Span-to-depth ratio was 4.0.

2.3. Testing of specimens

Due to highly brittle nature, testing of HSC in tension poses one major problem. The possibility of specimen failure at or near the grips, due to possible stress concentration effects and improper alignment of the specimen in the test setup. Special loading steel grips were fabricated for applying tensile loading on the specimens. The specimens were loaded at a constant rate of loading. At every load increment, the crack mouth opening displacement (CMOD) was measured at both the cracks of the specimen using linearly variable differential transducers (LVDT). In this study, an attempt has been made to investigate the size effect law in high-strength concrete on DENCTS, ECCS and TPB with geometrically similar ones.

Table 2: Mechanical properties of various concrete mixes-DENCTS

Mix	f _c MPa	E, GPa	f _t	f _{cr}
410-A	95.7	37.0	4.58	7.14
416-A	100.2	37.4	4.64	6.63
420-A	90.2	37.0	4.08	6.00
415-A	112.5	39.6	4.81	7.56
460-B	108.0	38.8	4.75	7.20
466-B	114.0	39.9	4.83	7.31
470-B	116.0	40.2	4.86	8.80
465-B	91.0	40.6	4.50	-----
510-C	93.5	39.0	4.84	7.26
516-C	95.0	39.0	5.06	7.11
520-C	85.0	40.9	4.41	9.34
515-C	85.0	43.7	4.88	8.72

3. TEST RESULTS AND DISCUSSION

3.1. Size effect in direct tension

Table 2 shows the mechanical and elastic properties of concrete in various concrete mix groups. Figure 1 shows a typical curve showing the variation of nominal strength with size of specimen. It has been

generally observed that in smaller size test specimens i.e. 80mm, the nominal strength has been higher, then decreasing trend has been followed up to 110 mm. As the size of specimen increases from 110 to 210 mm, the strength increases. The general size effect on test specimen has been observed when the specimen size is greater than 210 mm. The size effect plot, whether it is based on gross or net cross-sectional area appears to show one definite trend, viz. as the size increases after a certain characteristic dimension, the nominal strength decreases. The characteristic dimension here is 210 mm in HSC in direct tension, while it was 225 mm as observed by (Walsh 1976) in flexure. Quite interestingly, HSC shows a lesser characteristic dimension viz. 210 mm. It looks obvious because as the strength of concrete increases, it is supposed to be more brittle and naturally, this size should become pronounced at a lesser size. Based on the above facts, it may be said that brittleness or otherwise ductility of a structural element can be considered to be constituted by two sources. One source is the inherent material property and the other one is on account of the size. Inherently more brittle materials show size effect law at relatively smaller sizes, while relatively more ductile materials show the law at relatively larger sizes. In the limit, ideal brittle materials show size effect law at almost zero size, while ideally ductile materials show the law at infinite size. Weak size effect has been reported on the nominal strength of concrete and sandstone (van Vliet and van Mier 2000)). Bazant et al. (1991) reported that the nominal strength on split cylindrical specimens agrees with the general size effect law up to certain diameters, for larger sizes there appears to be deviation from the size effect law. It has been observed that the response of HSC has been very close to LEFM (Bazant and Schell 1993). A report on studies on HSC has been reported (Sener 1998).

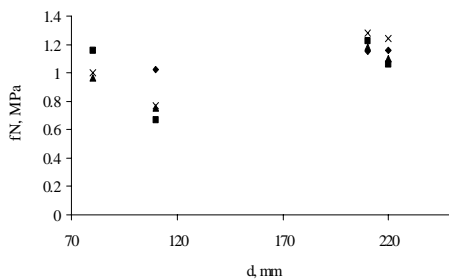


Figure 1: Nominal strength vs. size of test specimen-410-A to 415-A.

3.2. Size effect in eccentric compression

The variation of nominal strength of HSC with size of eccentric compact compression specimen (ECCS) on natural scale is shown in Figure 2. It demonstrates that the nominal strength decreases as the size of test specimen increases. The nominal strength is expressed as a function of the size of test specimen ($r = 0.94$) is given by

$$\sigma_N = 28.856 d^{-0.5665} \quad (2)$$

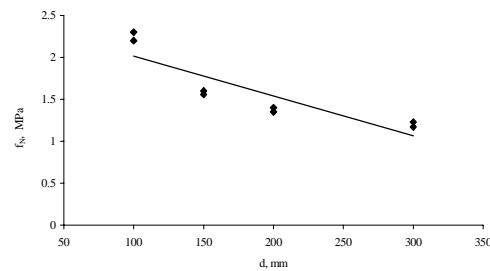


Figure 2: Nominal strength vs. size of test specimen using ECCS.

Figure 3 shows the variation of $\log(\sigma_N)$ with $\log(d)$. The nominal strength is related with the size of test specimen in the form of equation 3. The slope of the straight line is -0.5665 , which is very close to -0.5 . It indicates that the ECCS exhibits a behavior very close to LEFM.

$$\log(\sigma_N) = -0.5665 \log(d) + 1.46 \quad (3)$$

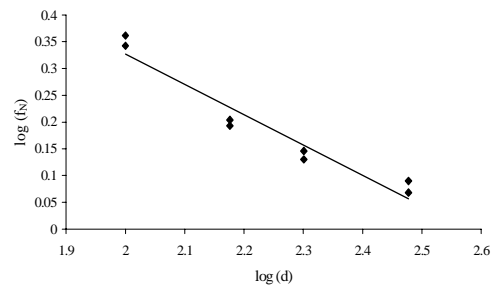


Figure 3: $\log(f_N)$ vs. $\log(d)$ in plain HSC on ECCS.

Strong size effect on the strength in HSC using ECCS has been observed. The Bazant's size effect law, in the linear form by rearranging the terms, is

$$\sigma_N = \frac{Bf_0}{\sqrt{1 + \frac{d}{d_0}}} \quad (4)$$

Where f_0 = tensile strength of concrete (MPa), d = size of specimen (mm), $d_0 = \lambda_0 d_a$, d_a = maximum size of coarse aggregate (mm), B = constant, λ_0 = constant.

After linearizing the size effect law in the form of $y = Ax + C$. Where $y = (f_0/\sigma_N)^2$, $x = (d/d_a)$. The tensile strength of the concrete was 5.0 MPa. Then the linear equation is

$$y = 1.20x + 0.14 \quad (5)$$

The constants are $A = 1.20$, $C = 0.14$, $B = 1/\sqrt{C} = 2.695$, $\lambda_0 = (C/A) = 0.1146$.

Then the nominal strength equation from the experimental data is given below;

$$\sigma_N = \frac{2.695f_0}{\sqrt{1 + 8.726\frac{d}{d_a}}} = \frac{13.475}{\sqrt{1 + 8.726\frac{d}{d_a}}} \quad (6)$$

And the ratio (σ_N/Bf_0) is

$$\frac{\sigma_N}{Bf_0} = \frac{1}{\sqrt{1 + 8.726\frac{d}{d_a}}} \quad (7)$$

Figure 4 shows the regression line with a slope of 1.20 and with a vertical intercept of 0.14. The regression coefficient is 0.97. The variation of the fit is shown in Figure 5. It shows that $\log(\sigma_N)$ vs. $\log(d/d_a)$ is a descending curve.

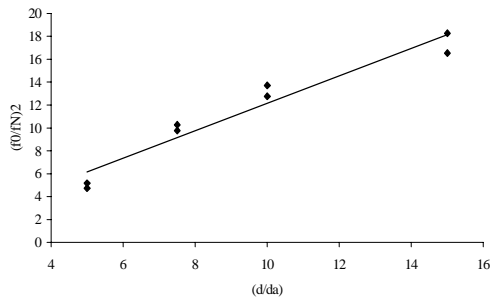


Figure 4: $(f_0/f_N)^2$ vs. (d/d_a) in HSC using ECCS.

3.3. Size effect in bending

The nominal strength, σ_N , of beam specimens was calculated by dividing the ultimate load by the gross area of cross section. The variation of nominal strength on three-point bend beam specimens (TPB), with size of test specimen on natural scale is shown in Figure 6.

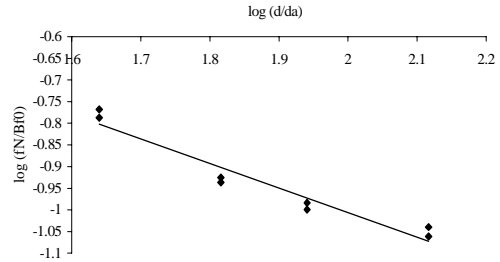


Figure 5: $\log(fN/Bf_0)$ vs. $\log(d/d_a)$ in ECCS.

It demonstrates that the nominal strength decreases as the size of test specimen increases. The nominal strength is expressed as a function of the size of test specimen, with a regression coefficient of 0.985, which is given by

$$\sigma_N = 0.755 - 0.0009(d) - 9 \times 10^{-6}(d^2) \quad (8)$$

Figure 7 shows the variation of $\log(\sigma_N)$ with $\log(d)$. A strong size effect on strength in HSC on TPB specimens has been observed. The slope of the descending line is -0.422 which is nearer to the value in LEFM i.e. -0.5 .

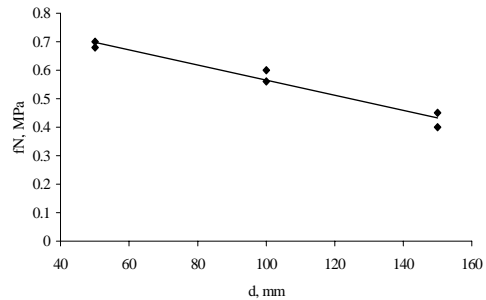


Figure 6: Nominal strength vs. specimen size in TPB.

It is worth comparing the descending branches of HSC with ECCS. It is -0.422 for TPB while it is -0.566 for ECCS, which obviously means that

latter is steeper than the former. It validates the relative brittleness of HSC with geometry. The expression is

$$\log(\sigma_N) = -0.422 \log(d) + 0.5696 \quad (9)$$

The comparison with the Bazant's size effect law (equation 1) can be written in the linear form by rearranging the terms. After linearizing the expression 10 in the form of $y = Ax + C$. Where $y = (f_0/\sigma_N)^2$, $x = (d/d_a)$. The tensile strength of the concrete was 5.0 MPa. Substituting the y and x from the experimental results, or in other words, substitute for σ_N and d from the results (f_0 and d_a are constants).

$$y = 10.914 x + 1.6825 \quad (10)$$

The constants obtained are $A = 10.914$, $C = 1.6825$, $B = 1/\sqrt{C} = 0.77$, $\lambda_0 = (C/A) = 0.154$.

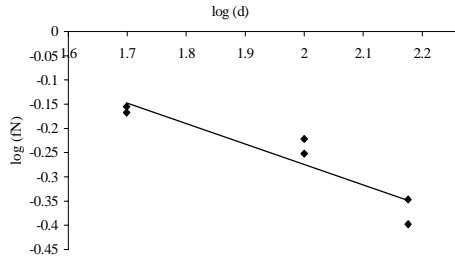


Figure 7: log (fN) vs. log (d)-TPB.

Then the nominal strength equation from the experimental data is given below

$$\sigma_N = \frac{0.77 f_0}{\sqrt{1 + 6.5 \frac{d}{d_a}}} = \frac{3.85}{\sqrt{1 + 6.5 \frac{d}{d_a}}} \quad (11)$$

And the ratio (σ_N/Bf_0) is

$$\frac{\sigma_N}{Bf_0} = \frac{1}{\sqrt{1 + 6.5 \frac{d}{d_a}}} \quad (12)$$

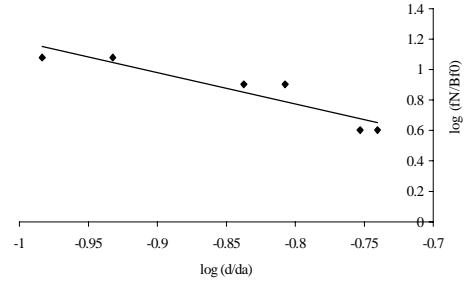


Figure 9: (fN/Bf0) vs.(d/da) in TPB.

Figure 8 shows the regression line with a slope of $A=10.91$ and with an intercept of $C=1.682$. The regression coefficient is 0.93. The variation of the fit is shown in Figure 9. It demonstrates that $\log(\sigma_N/Bf_0)$ versus $\log(d/d_a)$ is a descending curve, which indicates that the strong size effect law has been achieved in high strength concrete. However, it is less strong compared to that in ECCS. It demonstrates that the compact compression and the beam specimens exhibit size effect, while in the case of tension specimens, the size effect has not been conclusive. In the case of eccentric compression specimens, the variation of nominal strength with size of specimen has been quite close to the asymptote of slope $-1/2$ for linear elastic fracture mechanics, while for the case of tension specimen the curve is quite remote from this asymptote. For the three-point bend specimen an intermediate situation occurs. It has been observed that the size range of tension specimens would be increased about 20 times to approach the asymptote as closely as the compression specimen. The tension specimen by far is the best for exploring the behavior near the horizontal asymptote for the strength criterion, and the eccentric compression specimen is best for finding the linear fracture mechanics asymptote. In the case of eccentric compression specimen, the FPZ is very small. In tension specimen, the entire ligament length is in tension, which causes the FPZ to become very large. In the case of beam section, roughly half of the cross section is subjected to tension and half to compression, and the fracture process zone is of medium size. ECCS and TPB specimens showed relatively strong size effect, which was very close to the LEFM, while in direct tension it is negligible.

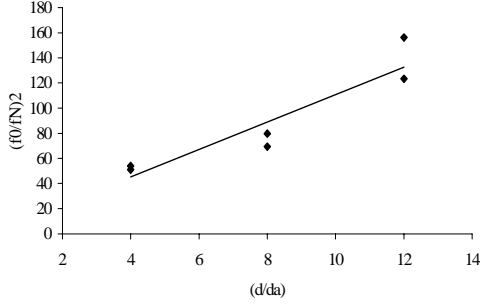


Figure 8: $(f_0/f_N)^2$ vs. (d/d_a) in TPB.

3.4. Size of fracture process zone

Fracture mechanics problems may be approached by dimensional analysis, a mathematical technique making use of the study of dimensions. Dimensional analysis is related to similitude; however, the approach is different. In dimensional analysis, from a general understanding of fracture phenomena, one first predicts the physical parameters that will influence the fracture, and then, by grouping these parameters in dimensionless combinations, a better understanding of the fracture phenomena is made possible. The size of fracture process zone in high-strength concrete is to be estimated from the experimental data using the various parameters of concrete. Visualizing the fracture problem considered in this study, it is intuitively adopted that strength of concrete is a significant parameter both in tension and compression. As the tensile strength is directly related to the compressive strength of concrete, only tensile strength of concrete is included in the analysis. Therefore this parameter should enter in to the fracture phenomena. The energy dissipated in creating fracture surfaces is one of the important parameters of the fracture problem. Above all, the size of non-homogeneity has very significant role to play in the size of damage in the region of crack tip. Because coarse aggregate is a major source of non-homogeneity, the maximum size of coarse aggregate is considered as one of the parameters. As has been reported and generally observed that the size of test specimen also influences the fracture process zone and ductility of concrete. Therefore, after judicious verification of the phenomena, the fracture problem must contain the fracture energy, G_F , strength of concrete and

modulus of elasticity, size of non-homogeneity and size of test specimen. Thus we can write

$$l_{fpz} = f(G_F, E, f_t, d_a, d) \quad (13)$$

l_{fpz} is the length of fracture process zone in concrete. The required expression may be conveniently assumed as a power equation as the fracture process zone significantly depends on the fracture energy, G_F , elastic modulus, E , size of non-homogeneity, d_a , the strength of concrete, f_t , and size of test specimen, d . The product of G_F and E divided by d is selected because l_{fpz} is directly related the amount of fracture energy G_F and inversely related to the size of test specimen.

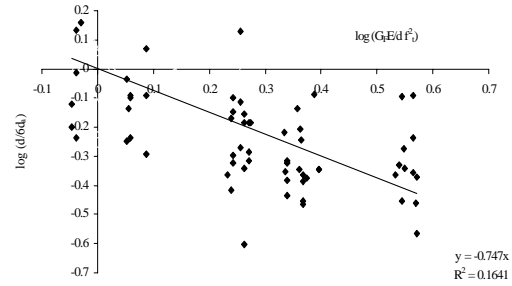


Figure 10: $\log(G_F E / d)$ vs. $\log(d/d_a)$.

$$l_{fpz} = (G_F E / d)^a (f_t)^b (d_a)^c \quad (14)$$

$$l_{fpz} = (G_F E / d)^a (f_t)^b (d_a)^c = d_a \quad (15)$$

The fracture process zone length for the lower bound solution is obtained at $a = 0$, $b = 0$ and $c = 1$. Substituting the values of $a = 0$, $b = 0$ and $c = 1$ in equation 15, we get

$$l_{fpz} = (G_F E / d)^0 (f_t)^0 (d_a)^1 = d_a$$

To obtain the size of FPZ for any value of “a, b and c”, substitute these values in equation 15. This equation incorporates all the possible parameters, which influence the fracture phenomena. Hence it is reasonable to incorporate the above parameters for the study of fracture process zone in high-strength concrete. In the present case, $a = 1$, $b = -2$ and $c = 1$ are adopted to estimate the values of the size of FPZ. In order to obtain the upper bound

solution, substitute $b = -2a$ and $c = 1$ to obtain the value of “a”. Equation 16 becomes

$$l_{fpz} = \left[\frac{G_F E}{df_t^2} \right]^a (d_a) \quad (16)$$

But l_{fpz} cannot be greater than the uncracked ligament length of the specimens for the upper bound value. In the present case, in DENCTS, the maximum size of FPZ can be $d/6$. The value of “a” can be obtained for limiting value of FPZ in concrete. Then the value of “a” is given by

$$l_{fpz} = \left[\frac{G_F E}{df_t^2} \right]^a (d_a) = \frac{(d - 2(\frac{d}{3}))}{2} = \frac{d}{6} \quad (17)$$

$$a \log \left[\frac{G_F E}{df_t^2} \right] = \log \left[\frac{d}{6d_a} \right] \quad (18)$$

It clearly demonstrates that the value of constant “a” varies with the size of specimen, size of coarse aggregate, G_F , E and f_t . The value of “a” is a function of the size of specimen. The plot of “log ($d/6d_a$) vs. log ($G_F E/df_t^2$)” is shown in Figure 10, the solution for “a” is -0.747 .

The length of fracture process zone in all the test specimens is calculated using the Equation 20.

$$a = \frac{\log \left[\frac{d}{6d_a} \right]}{\log \left[\frac{G_F E}{df_t^2} \right]} \quad (19)$$

The size of FPZ ranges between 8 mm and 56mm.

$$l_{fpz} = \left[\frac{G_F E}{df_t^2} \right]^{-0.747} (d_a) \quad (20)$$

4. CONCLUSIONS

The nominal stress at peak in HSC using DENCTS tends to decrease as the size of specimen increases after certain minimum size. Such a minimum size could be called characteristic size because it could be characteristic of the type of the material. The characteristic size also varies with the type of test. For example, in the present case for HSC of strength

greater than 75 MPa and less than 115 MPa, it could be 210 mm under direct tension. Size effect has been observed in HSC on both ECCS and TPB specimens. Due to the unconstraining region in tension, the size of FPZ might be so high that the application of LEFM to DENCTS requires huge test specimen sizes. The size of the estimated FPZ evaluated using the proposed expressions range between 8mm and 56mm. Very strong size effect has been observed on HSC using ECCS and TPB with a small size of test specimens.

5. REFERENCES

- Bazant, Z.P. Kazemi, M.T. Hasegawa, T., and Mazars, J. 1991. Size effect in brazilian split- cylinder tests: measurements and fracture analysis”, *ACI Materials Journal*, 88(3): 325-332.
- Bazant, Z.P. and Oh. 1984. Size effect in blunt fracture: concrete, rock, metal”, *Journal of Engineering Mechanics*, 110 (4): 518-535.
- Bazant, Z.P. Ozbolt, J. and Eligehausen, R. 1994. Fracture size effect: review of evidence for concrete structures”, *Journal of Structural Engineering*. 120(8): 2377- 2398.
- Hillerborg, A. Modeer, M. and Petersson, P.E. 1976. Analysis of crack formation and crack growth in concrete by means of fracture mechanics and finite elements”, *Cement and Concrete Research*, 6(6): 773-782.
- Jeng, Y. and Shah, S.P. 1985. Two-parameter fracture model for concrete. *Journal of Engg. Mech.*, 111(10): 1227-1240.
- Karihaloo, B.L. 1995. *Fracture mechanics and structural Concrete*”, Longman Scientific & Technical, USA.
- Sener, S. 1998. Size effect tests on high strength concrete”, *Journal of Materials in Civil Engineering*, 46-48.
- van Vliet, M.R.A. and van Mier. 2000. Experimental investigation of size effect in concrete and sandstone under uniaxial tension”, *Engineering Fracture Mechanics*. 65: 165-188.
- Walsh, P.F. 1976. Crack initiation in plain concrete. *Magazine of Concrete Research*. 28(94): 37-41.